Development of an atmospheric Cherenkov imaging camera for the CANGAROO-III experiment

S. Kabuki, K. Tsuchiya, K. Okumura, R. Enomoto, T. Uchida, and H. Tsunoo
Institute for Cosmic Ray Research, University of Tokyo, 5-1-5 Kashiwa-no -Ha, Kashiwa City,Chiba 277-8582, Japan
Shin. Hayashi, Sei. Hayashi, F. Kajino, A. Maeshiro, and I. Tada *Department of Physics, Konan University,Hyogo 658-8501, Japan*
C. Itoh *University of Ibaraki, Mito, Ibaraki 310-8512, Japan*
and CANGAROO collaborators

Abstract

A Cherenkov imaging camera for the CANGAROO-III experiment has been developed and install for observations of gamma-ray induced air-showers at energies from 10^{11} to 10^{14} eV. The camera consists of 427 pixels, arranged in a hexagonal shape at 0.17° intervals, each of which is a 3/4-inch diameter photomultiplier module with a Winston-cone–shaped light guide. The camera was designed to have a large dynamic range of signal linearity, a wider field of view, and an improvement in photon collection efficiency compared with the CANGAROO-II camera. The camera, and a number of the calibration experiments made to test its performance, are described in detail in this paper.

Introduction

CANGAROO-III, the next phase of the project, aims at the detection for gamma-rays at energies of 0.1∼100 TeV (1TeV=10^{12}eV) using four 10-meter-diameter telescopes for stereoscopic reconstruction of atmospheric Cherenkov shower images. Various improvements in the design of the imaging Cherenkov camera have been made for the CANGAROO-III experiment(detail can be found in [4]).

The technique of stereoscopic observing [2], allows more precise measurements to be made: a significant improvement in the separation efficiency of gamma-ray events from the cosmic-ray background, a more precise reconstruction of the arrival direction determined on an event-by-event basis [1], and an improvement in the energy resolution of up to 20% [3]. The stereoscopic technique is effective for both point-like sources and for extended gamma-ray sources, such as supernova remnants.

pp. 1–6

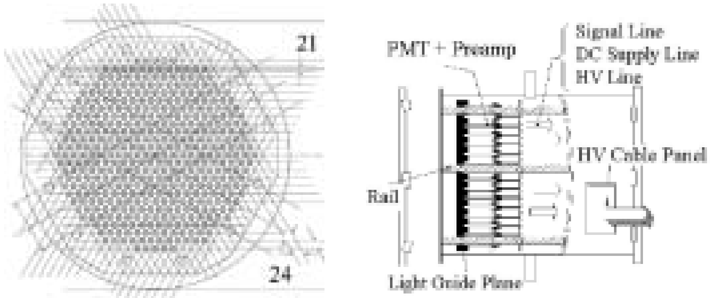

Fig. 1. Schematic design of the CANGAROO-III camera frame. The left figure shows the front view and the right figure shows a side view of the camera. The camera pixels are arranged on a hexagonal grid, as shown in the left figure.

In this paper, the development of the Cherenkov imaging camera for the second CANGAROO-III telescope is described. Detailed studies were made concerning the number, size, type and arrangement of photomultiplier tubes, the preamplifier circuits, the light guides, reliable calibration sources and the overall performance of the camera system.

1. Camera design

1.1. Structure

The camera design of the second CANGAROO-III telescope was made based on the above requirements. A schematic diagram of the camera structure is shown in Fig. 1.

The camera is contained in a cylindrical vessel of 800 mm in diameter and 1000 mm in length, which provides shielding from both rain and light. The vessel is made of an aluminum alloy (A5052) in order to reduce the weight and provide sufficient rigidity. Inside the camera vessel, 427 PMT modules, regulator circuit panels, an LED (light emitting diode) light diffuser for gain calibration, and several other instruments such as a thermometer, are contained. The camera frame consists of two aluminum templates (5 mm in thickness), in which holes (21 mm in diameter) are drilled at locations corresponding to each of the 427 pixels, as shown in Fig. 1. (left). Every PMT module, consisting of an PMT and a preamplifier (20.5 mm in diameter), is held by these templates. Light guides are attached to the front panel. The photocathode plane of the PMT module is held close to the back plane of the light guide. The front panel, on which the light guides are attached, is fixed at the focal plane. All segmented mirrors can be seen from every pixel position.

The pixels are arranged in hexagonal shape in order to maximize the collection efficiency of the Cherenkov light. The pixel size was determined to be 0.17 degrees from a simulation study [2], taking into account the spot size of the 10 m composite mirror [5].

1.2. PMT module

It is cylindrical with a diameter of 20.5 mm and length of 173.5 mm. Three types of cable (the signal, the D.C. power and the high voltage supply) are passed through from the back end of the module. The module consists of a 19 mm (3/4 inch) PMT (Hamamatsu R3479UV), bleeder circuits and a pre-amplifier which are attached at the base of the PMT. An operational amplifier (MAX4107) is used as the pre-amplifier and the input signal from the PMT is amplified by a factor of 60. Each module is shielded with μ-metal (0.2 mm thick) to reduce any effect due to the geomagnetic field and cross-talk between PMT modules. Each module (without cables) weighs 75 g.

1.3. Light-guide

The camera consists of PMTs with a significant amount of dead space between them, amounting to $\sim$65% of the total surface area. Light-guides reflect photons which would otherwise be incident upon the dead space onto to the photocathode area of the PMTs, thus increasing the light-collection efficiency. Another advantage is that light-guides reduce the background of photons coming from outside of the mirrors, i.e., at a shallow angles with respect to the light-guide plane.

After Monte Carlo simulations for various shapes of light guides were performed to evaluate their performance, the optimal shape of the light guide was determined. The most efficient light guide design was based on the Winston cone([6],[7].), but with a hexagonal entrance shape.

2. Calibration light source

To monitor the gain of the whole camera system over the longer term, a new compact monitor system(shown in Fig. 2.) was developed for the camera vessel, consisting of an LED and a specially patterned screen to diffuse the light uniformly to every pixel. The absolute number of photoelectrons by the PMTs can be calculated from the widths of the distributions of the output charges from the PMTs based on Poisson fluctuations. Using this device and method, the gain of every PMT can be obtained precisely. The high uniformity of light over the camera surface has the advantage of reducing the calibration time. As this device

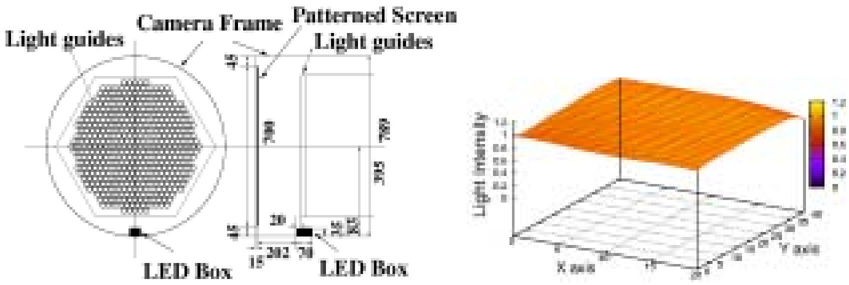

Fig. 2. Left: Conceptual figure of the camera LED system, which consists of a light source (LED box) and a patterned screen installed in the camera vessel. Right: Light intensity at the surface of the patterned screen over an area of 20 cm $\times$ 40 cm. The average deviation from uniformity was measured to be 2.6%.

is used when the camera lid is closed, these operations can be carried out even during the day. Light intensity at the surface of the patterned screen over an area of 20 cm $\times$ 40 cm. The average deviation from uniformity was measured to be 2.6%.

3. Calibration

3.1. PMT module performance

Before the camera was constructed, the characteristics of all PMT modules were calibrated individually and the results were stored in a database.

The HV was adjusted to give a gain of 1.21×10^7 (including the preamplifier gain) measuring the single-photon spectrum. The typical distribution of a single photoelectron peak is shown in Fig. 3. The peak due to a single photon signal can be cleanly separated from background. The linearity of all the PMT module was mesured at gain 1.21×10^7. The amount of the light was changed to be 1, 10, 50, 100, 210, 280, 350, 500, 700, and 1000 p.e.. Data points were fitted using the following empirical formula:

$$F(x) = \begin{cases} x & (x \leq a) \\ \frac{((x-a+c)^b - c^b)}{b} c^{(1.0-b)} + a & (x > a), \end{cases}$$

where a approximately corresponds to the turning point of the line. The resulting average and standard deviation of a were 202.1 ± 12.7 (1σ) p.e.. The deviation from a linear line at 250 p.e. of the input light was estimated to be -5.1 ± 2.0 (1σ) % . The high-voltage dependence of the gain was measured with the amount of 10 p.e.

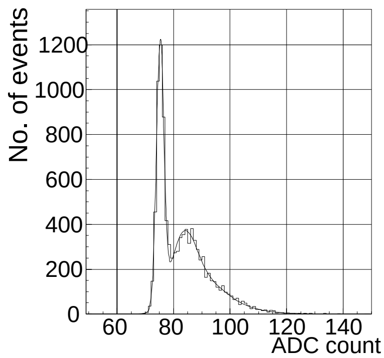

Fig. 3. Distribution of the single-photoelectron peak measured by a PMT module.

input. The gain was measured at HVs of 1100, 1200, 1300, 1400 and 1450 V, and fitted to the following formula:

$$(\text{Gain}) = K \cdot V^{\alpha},$$

The parameter α represents the gain sensitivity for the high voltage, and the average value for all modules was 4.9 ± 0.1. The timing resolution at 20-p.e. of input light for all PMT modules was 0.96 ± 0.09 nsec. The Quantum efficiency are measured for 10 out of 450 PMTs as function of the wavelength. The average of the quantum efficiency was estimated to be 25.0 ± 1.4 % at 400nm.

3.2. Performance of whole camera system

The uniformity of gain is measured with the diffused LED light source located 8m away. The average ADC/skb(skb: blue sensitivity) was a devitaion of 11%. The cross-talk effect among the neighboring pixels was investigated by illuminating one PMT module located at the center of the camera with an LED (at about 100 p.e. level). Cross-talk is measured to be less than 0.4%. The efficiency of the light acceptance was defined from the difference of ADC counts measured with and without light guides after a correction of the difference of the front/back area of the light guides, which is calculated as follows:

$$\text{Efficiency} = \frac{\text{ADC}_1}{\text{ADC}_2} / \frac{S_1}{S_2},$$

where ADC_1 (ADC_2) is the ADC counts with (without) the light-guide, and S_1 and S_2 are the area size of the front and back planes of the light guides (S_1/S_2=2.57), respectively. The absolute efficiency of measurement was adjusted to that of the simulation at 0° incident angle. The light correction efficiency is was confirmed to be consistent with the design value.

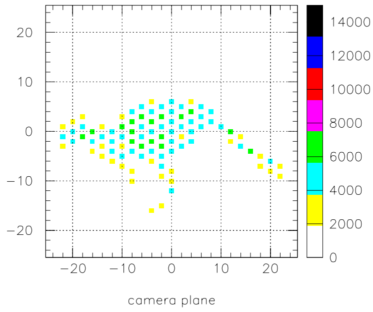

Fig. 4. Kangaroo image by our new camera.

The Kangaroo image of new camera is shown in Fig. 4. This image show the good performance of new camera.

Conclusion

The performance of the Cherenkov imaging camera for the second CANGAROO-III telescope was improved over that of the first (CANGAROO-II) telescope with respect to the uniformity of gain, timing resolution and the light-collection efficiency. The 427 PMTs have been carefully calibrated and the results stored in a database so that the camera performance can be optimized. This camera performance is suitable for observations with the next generation of gamma-ray telescopes.

References

[1] Akerlof C.W. et al. 1991, Astrophys. J. 377, L97.

[2] Enomoto R. et al. 2002, Astropart. Phys. 16, 235.

[3] Hoffman W. 1997, in Proc. Towards a Major Atmospheric Cherenkov Detector V, (Kruger Park, South Africa) p.284.

[4] Kabuki S. et al. 2002, ICRR-Report-493-2002-11, submitted for publication.

[5] Kawachi A. et al. 2001, Astropart. Phys., 14, 261.

[6] Winston R., & J. O'Gallagher 1983, Int. Journal of Ambient Energy 4, 171.

[7] Winston R. 1991, Scientific American 264 no.3, 52.